International Journal of Applied Engineering Research ISSN 0973-4562 Volume 10, Number 13 (2015) pp 33452-33456

Induction Motor Bearing Fault Detection Using Hybrid Kurtosis-Based Method

Mohd Sufian Othman[1], Mohd Zaki Nuawi[1*] and Ramizi Mohamed[2]

[1]Department of Mechanical and Material Engineering
[2]Department of Electrical, Electronic and Systems Engineering
Universiti Kebangsaan Malaysia, 43600 Bangi, Selangor, Malaysia
sufian@jkr.gov.my, [*]zaki@eng.ukm.my, ramizi@eng.ukm.my

Abstract
Wide usage of induction motors in industries and domestics demand a fast and reliable condition monitoring method to make sure no interruption in operation and also to prevent catastrophic damages which are costly and time consuming. Bearing, the most fragile part in induction motor has become a prominent subject recently. Vibration and AE measurement are popular methods in bearing fault detection. However, the combination of both signals in an analysis still very few in the literature. Hence, in the present study, a hybrid kurtosis-based method was proposed to analyse simultaneous vibration and AE signal for identification of bearing faults, i.e. inner race, and outer race. Comparison with classical methods, i.e. kurtosis and envelope spectrum analysis also discussed. The results show that the proposed system able to detect inner race and outer race defected bearings in 4 poles and 2 poles induction motor.

Keywords Condition monitoring, statistical analysis, kurtosis, hybrid I-kaz;

Nomenclatures

AE	Acoustic emission
f_{IR}	Inner-race fault frequency
f_{OR}	Outer-race fault frequency
I-kaz	Integrated kurtosis-based algorithm for Z-Filter
IRF	Inner race faulty bearing
Kur	Kurtosis
N	Number of samples
NB	Normal bearing
ORF	Outer race faulty bearing
rpm	Revolutions per minute
s	Standard deviation
V	Vibration
Z_h^{∞}	Hybrid I-kaz coefficient

Introduction

Three phase induction motor is the most popular electrical machine in industrial application because of its simplicity, robustness, ruggedness, reliability, and economical. This type of motor has also been used in domestic appliances, e.g. the front loading and the top loading washing machine drives [1]. Although this electromechanical device is highly reliable, it still vulnerable to many type of faults sources from mechanical and electrical stresses during operation [2]. One of critical components in induction motor is bearing, reported to be the most fragile part which can lead to catastrophic failure [3], [4]. The deep groove ball bearing is the most common form of rolling bearing used in induction machine. Fig. 1 shows the nomenclature of single row deep groove ball bearing, being the subject of this study.

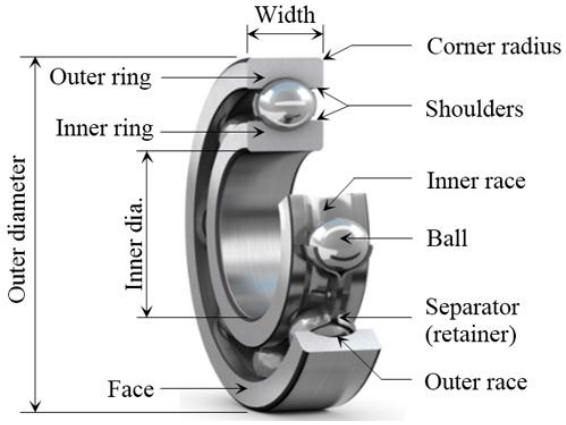

Figure 1: Nomenclature of a deep groove ball bearing [5].

Common causes of bearing failures are overloading, contamination, improper lubrication, and misalignment [6]. Most of the failures occurred on outer race and inner race, location where the balls hit and roll each time the bearing are moving. For decades, development of bearing condition monitoring technique became a crucial topic, with vibration and acoustic measurement are among established methods [7]. Although vibration is the most popular tool [8], acoustic emission (AE) was reported to be more efficient in early detection of bearing faults [9]. AE is defined as elastic waves generated by the rapid release of energy from sources within a material, was introduced as a non-destructive testing method by J. Kaiser in 1950 [10].

Signal data can be analysed in time domain, frequency domain, or a combination of both. In time domain, kurtosis method is one of earliest approach in bearing fault detection, first proposed by Dyer and Steward in 1978 [11]. Since then, kurtosis gains widespread usage and have been applied in more advanced techniques such as spectral kurtosis and

kurtogram [12]–[14]. Kurtosis also have been used in feature extraction for modern artificial intelligence techniques, i.e. neural network, fuzzy logic, and expert system [15]–[17]. Moreover, time domain data can be transformed into the frequency domain. In frequency domain, envelope analysis or also known as high frequency resonance technique is well known method, applied successfully in industrial application [18].

Hybrid I-Kaz Method

I-kaz is a statistical based method using the graphical plot to show the scatteredness of data distribution about its centroid and the numerical descriptor called I-kaz coefficient [19]. I-kaz method has been applied successfully in bearing condition monitoring [20], [21]. Inspired from I-kaz, the hybrid I-kaz also provides similar outputs, but using the combined signal data. This method has been utilized in automotive suspension system analysis using strain and vibration signals [22], [23].

For a combination of vibration and AE signal, hybrid I-kaz coefficient can be defined as:

$$Z_h^{\infty} = \frac{1}{N}\sqrt{Kur_V \cdot {s_V}^4 + Kur_{AE} \cdot {s_{AE}}^4}\,. \qquad (1)$$

where N is number of samples, Kur_V and Kur_{AE} are kurtosis of vibration and AE signal, and s_V and s_{AE} are standard deviation of vibration and AE signal, respectively.

In this paper, we demonstrate the usage of hybrid I-kaz method with combined signals of vibration and AE to detect bearing faults in 4 poles and 2 poles induction motor. Comparison with the kurtosis method in time domain, and the envelope analysis in frequency domain also discussed.

Methodology

The test rig used during this research work consists of a two-speed pole-changing squirrel cage induction motor, with the drive-end ball bearing was under test. Three bearing conditions were tested, i.e. (1) normal, (2) inner race fault, and (3) outer race fault. All defected bearings were artificially damaged by axially drilled of 1 mm hole through its raceway. The motor was coupled with tacho generator and magnetic powder brake through elastic couplings.

Vibration signal was collected using an accelerometer with sensitivity of 100 mV/g, and an AE transducer with sensitivity of 100 V/µm was used to measure AE signal. Accelerometer and AE transducer were mounted on motor housing at radial and axial position respectively, close to test bearing location using special adhesive glue. All sensors were connected to oscilloscope and linked to the computer. Detail layout for the test rig setup is shown in Fig. 2.

The motor was running using 4 poles and 2 poles connection, tested repeatedly for each bearing condition with no load applied (Refer Fig. 3). The measured speed for 4 poles and 2 poles were 1450 and 2950 rpm respectively. The measurements were carried by 32 consecutive acquisitions, each having a sampling period of 1 s at a sampling frequency of 47,988 Hz, saved separately using PicoScope Software version 6.10.16. Hence, a total number of 3,198,976 samples were recorded in 32 files for each condition.

Table 1: Test Bearing Specification

Bearing code	Outer dia.	Inner dia.	Width	Ball dia.	Number of balls
FAG 6204ZR C3	47 mm	20 mm	14 mm	7.938 mm	8

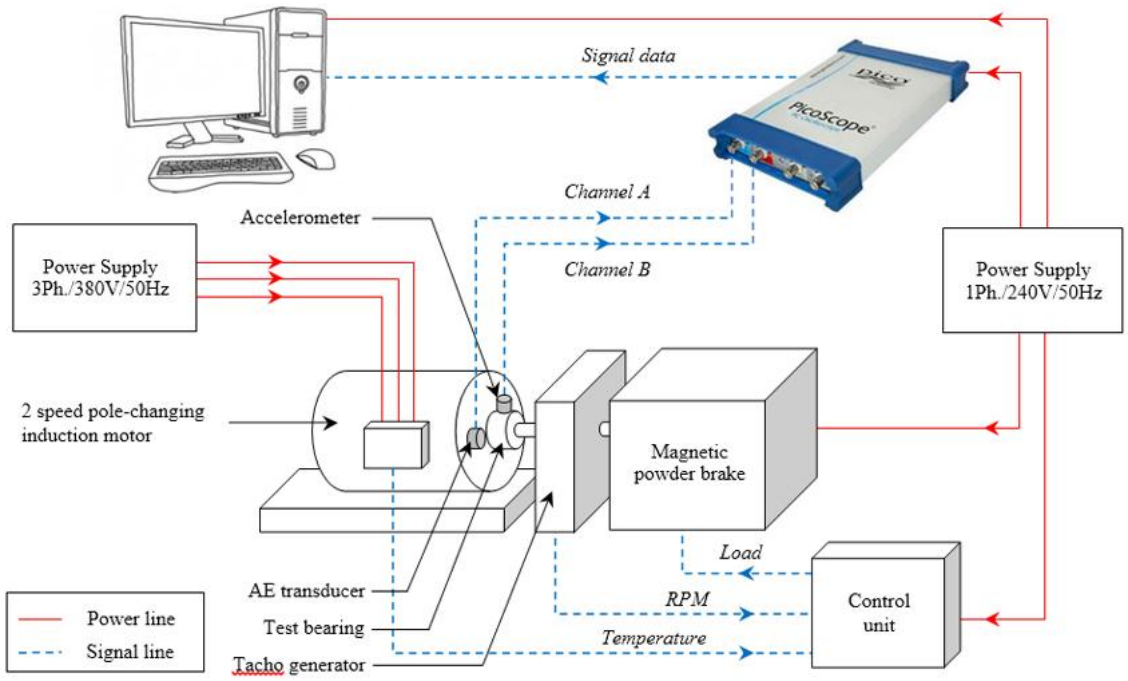

Figure 2: Experimental test bench layout.

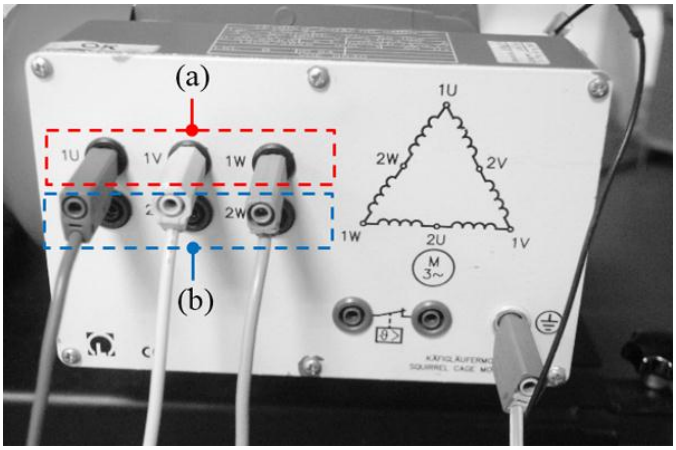

Figure 3: Motor connection: (a) 4 poles, and (b) 2 poles.

Results and Discussion

The collected data have been analysed in MATLAB version 8.3 using three methods: i.e. (1) hybrid I-kaz, (2) kurtosis, and (3) envelope spectrum. The following show results for the first segment of 1 s out of 32 s.

Hybrid I-kaz Analysis

Comparison of hybrid I-kaz analysis between normal, outer race fault, and inner race fault bearing are shown in Fig. 4 and Fig. 5 for motor running at 1450 rpm and 2950 rpm respectively. Clear differences are observed in graphic plots of faulty bearings compared to normal bearing in both figures. The hybrid I-kaz coefficient (Z_h^∞) of faulty bearings in 1450 rpm (Fig. 4) were significantly larger than normal bearing, i.e. 1.42×10^{-7} for inner race fault and 1.12×10^{-6} for outer race fault, compared to 1.50×10^{-8} in normal bearing. However, difference of Z_h^∞ between normal and faulty bearings in 2950 rpm (Fig. 5) were higher than in 1450 rpm, i.e. 2.22×10^{-6} for inner race fault and 1.17×10^{-5} for outer race fault, compared to 7.59×10^{-8} in normal bearing.

Analysis of the scatteredness of hybrid I-kaz against kurtosis for acceleration and AE signal from all 32 files are presented in Fig. 6 and Fig. 7, for 1450 and 2950 rpm respectively. Clear difference between normal and faulty bearing data was observed in both figures for the acceleration and the AE signals. Data were concentrated at the same location for normal bearing, but scattered with different patterns for faulty bearings. For acceleration signal, inner race fault shown a high positive correlation between hybrid I-kaz and kurtosis value, but for the outer race fault, no specific correlation was observed. However, for AE signal, both inner race and outer race faults shown low positive correlations between hybrid I-kaz and kurtosis.

Comparison with Kurtosis Method

Comparison of kurtosis analysis between acceleration and AE signal data for motor running at 1450 and 2950 rpm are presented in Fig. 8 and Fig. 9 respectively.

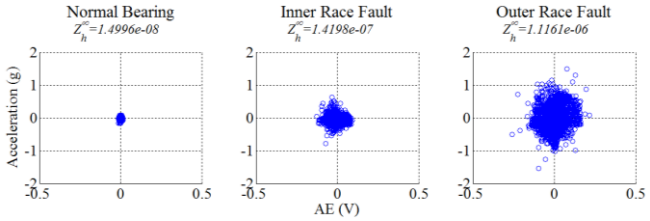

Figure 4: Comparison of hybrid I-kaz (acceleration vs AE) for motor at 1450 rpm.

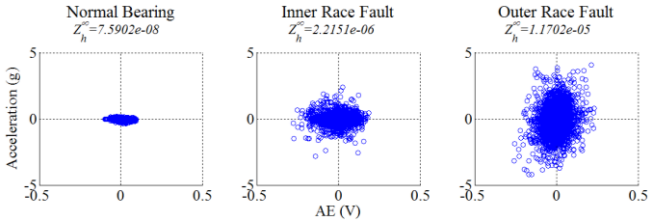

Figure 5: Comparison of hybrid I-kaz (acceleration vs AE) for motor at 2950 rpm.

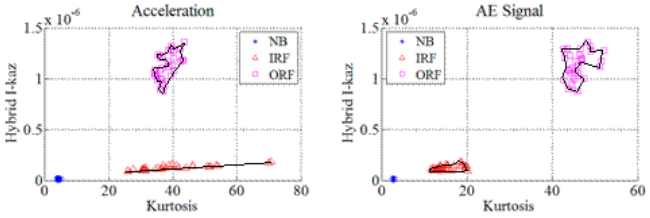

Figure 6: Scatter plots for hybrid I-kaz vs kurtosis of acceleration and AE signal at 1450 rpm.

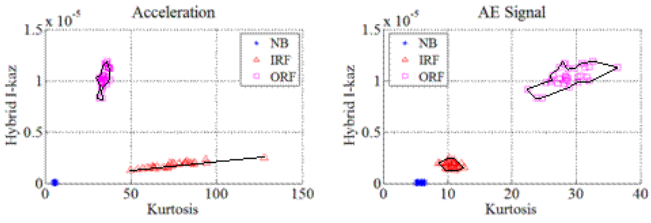

Figure 7: Scatter plots for hybrid I-kaz vs kurtosis of acceleration and AE signal at2950 rpm.

At 1450 rpm, kurtosis values from both vibration and AE signals verified bearing conditions accordingly. Kurtosis of acceleration and AE signals for normal bearing were closed to 3 and for faulty bearings, all kurtosis were significantly higher with the highest value of acceleration signal was from the inner race faulty bearing and for the AE signal was the outer race faulty bearing.

Same finding also observed in 2950 rpm result (see Fig. 9). Although kurtosis for the normal bearing was slightly higher than 3, kurtosis for all faulty bearings were significantly higher. The highest value for acceleration and AE signal remained the same as what was found in 1450 rpm.

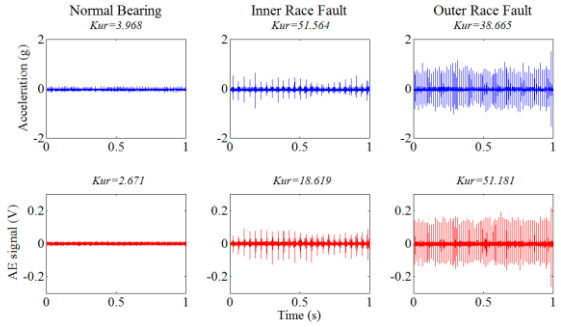

Figure 8: Comparison of acceleration and AE waveform for motor at 1450 rpm.

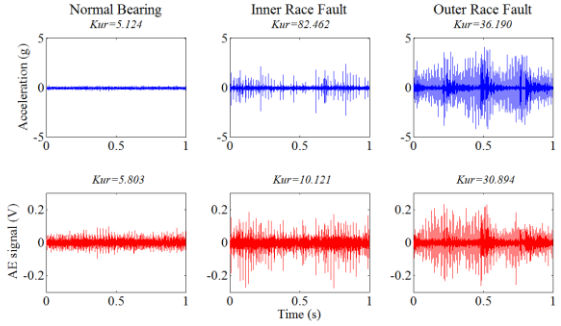

Figure 9: Comparison of acceleration and AE waveform for motor at 2950 rpm.

Comparison with Envelope Analysis

Comparative study of the envelope spectrum for 1450 rpm and 2950 rpm are presented in Fig. 10 and Fig. 11 respectively. Vertical lines indicated harmonic fault frequencies have been added to the inner race fault and the outer race fault plots. Fault frequencies for both rotational speeds are shown in Table 2.

Table 2: Test Bearing Fault Frequencies in Hertz (Hz).

Fault Frequency	1450 rpm	2950 rpm
Inner race fault, f_{IR}	119.6	243.2
Outer race fault, f_{OR}	73.8	150.1

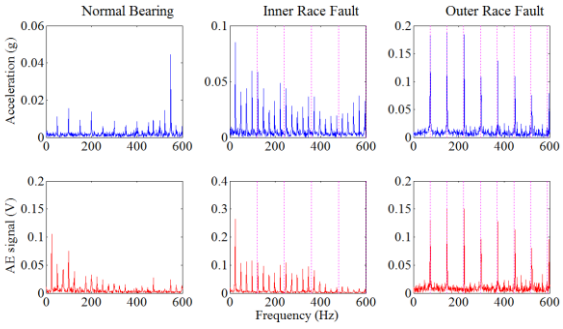

Figure 10: Comparison of acceleration and AE envelope spectrum for motor at 1450 rpm.

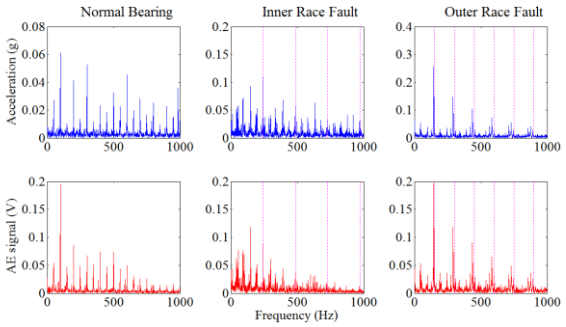

Figure 11: Comparison of acceleration and AE envelope spectrum for motor at 2950 rpm.

For outer race faulty bearing data at 1450 rpm (see Fig. 10), both vibration and AE signal spectrum indicated peak magnitudes arose at same harmonic fault frequencies, although were slightly shifted above calculated values at higher harmonic orders. Peak magnitudes in inner race fault, however, haven't appeared in same pattern, although the first harmonic can be detected. There are so many other spikes in between inner race harmonic fault frequencies.

Same pattern also observed in 2950 rpm for outer race fault, but signal magnitudes were decreased in higher frequencies. Only the first harmonic frequency was appeared exactly at its location, others were shifted just below the calculated values. However, for inner race fault, all harmonic frequencies found exactly at calculated values. Small variances from calculated values were observed at some harmonic fault frequencies might be caused by uneven balls dimension, unstable motor rotating speed, or changes in contact angles [24].

Conclusion

Based on experimental finding, the hybrid I-kaz method is suitable for detecting inner race and outer race fault in both 4 poles and 2 pole induction motor, especially when normal bearing data also available. In comparison with classical methods, vibration signal was provided highest kurtosis value in inner race fault, but the highest kurtosis value of AE signal was detected in outer race fault. In envelope analysis, same pattern was observed in both signals of outer race fault, but better identification of inner race fault harmonic frequencies were observed in the 2 pole motor with rotational speed of 2950 rpm.

References

[1] H. S. Rajamani and R. A. McMahon, "Induction motor drives for domestic appliances," *IEEE Industry Applications Magazine*, pp. 21–26, 1997.

[2] V. T. Tran, R. Cattley, A. Ball, B. Liang, and S. Iwnicki, "Fault diagnosis of induction motor based on a novel intelligent framework and transient current signals," *Chem. Eng. Trans.*, vol. 33, pp. 691–696, 2013.

[3] Motor Reliability Working Group, "Report of large motor reliability survey of industrial and commercial installations, Part 1," 1985.

[4] Motor Reliability Working Group, "Report of large motor reliability survey of industrial and commercial installations, Part 2," 1987.

[5] R. G. Budynas and J. K. Nisbett, *Mechanical Engineering Design*, 8th ed. McGraw-Hill, 2006.

[6] X. Jin, M. Zhao, T. W. S. Chow, and M. Pecht, "Motor bearing fault diagnosis using trace ratio linear discriminant analysis," *IEEE Trans. Ind. Electron.*, vol. 61, no. 5, pp. 2441–2451, 2014.

[7] N. Tandon and A. Choudhury, "A review of vibration and acoustic measurement methods for the detection of defects in rolling element bearings," *Tribol. Int.*, vol. 32, no. 8, pp. 469–480, 1999.

[8] L. Batista, B. Badri, R. Sabourin, and M. Thomas, "A classifier fusion system for bearing fault diagnosis," *Expert Syst. Appl.*, vol. 40, no. 17, pp. 6788–6797, Dec. 2013.

[9] M. Kedadouche, M. Thomas, and A. Tahan, "Cyclostationarity applied to acoustic emission and development of a new indicator for monitoring bearing defects," *Mech. Ind.*, vol. 15, no. 6, pp. 467–476, 2014.

[10] C. J. Hellier, "Introduction to nondestructive testing," in *Handbook of Nondestructive Evaluation*, 2003, pp. 1.1–1.27.

[11] D. Dyer and R. Stewart, "Detection of rolling element bearing damage by statistical vibration analysis," *J. Mech. Des.*, vol. 100, no. 2, pp. 229–235, 1978.

[12] B. Eftekharnejad, M. R. Carrasco, B. Charnley, and D. Mba, "The application of spectral kurtosis on Acoustic Emission and vibrations from a defective bearing," *Mech. Syst. Signal Process.*, vol. 25, no. 1, pp. 266–284, 2011.

[13] X. Zhang, J. Kang, L. Xiao, J. Zhao, and H. Teng, "A New Improved Kurtogram and Its Application to Bearing Fault Diagnosis," *Shock Vib.*, vol. 2015, p. 22 pages, 2015.

[14] D. Wang, P. W. Tse, and K. L. Tsui, "An enhanced Kurtogram method for fault diagnosis of rolling element bearings," *Mech. Syst. Signal Process.*, vol. 35, no. 1–2, pp. 176–199, 2013.

[15] A. K. Mahamad and T. Hiyama, "Fault classification based Artificial Intelligent methods of induction motor bearing," *Int. J. Innov. Comput. Inf. Control*, vol. 7, no. 9, pp. 5477–5494, 2011.

[16] W. Du, J. Tao, Y. Li, and C. Liu, "Wavelet leaders multifractal features based fault diagnosis of rotating mechanism," *Mech. Syst. Signal Process.*, vol. 43, no. 1–2, pp. 57–75, Feb. 2014.

[17] Z. Xu, J. Xuan, T. Shi, B. Wu, and Y. Hu, "Application of a modified fuzzy ARTMAP with feature-weight learning for the fault diagnosis of bearing," *Expert Syst. Appl.*, vol. 36, no. 6, pp. 9961–9968, Aug. 2009.

[18] D. Howieson, "Vibration Monitoring: Envelope Signal Processing," *Diagnostic Instrumentation, Inc.*, p. 14, 2003.

[19] M. Z. Nuawi, M. J. M. Nor, N. Jamaludin, S. Abdullah, F. Lamin, and C. K. E. Nizwan, "Development of integrated Kurtosis-based Algorithm for Z-filter technique," *J. Appl. Sci.*, vol. 8, no. 8, pp. 1541–1547, 2008.

[20] M. J. Ghazali, M. Z. Nuawi, and N. I. I. Mansor, "Low Cost Wear Monitoring of Bearing Shell in Connecting Rod via I-kaz Method," *Adv. Mater. Res.*, vol. 76–78, pp. 702–707, 2009.

[21] M. Z. Nuawi, S. Abdullah, a R. Ismail, and N. F. Kamaruddin, "A Novel Analysis (I-KAZ 3D) for Three Axial Vibration Signal in Bearing Condition Monitoring," in *7th WSEAS International Conference on System Science And Simulation In Engineering (ICOSSSE '08)*, 2008, pp. 318–322.

[22] S. Abdullah, M. Z. Nuawi, M. Z. Nopiah, and A. Ariffin, "Study on correlation between strain and vibration signal using hybrid I-Kaz method," *Contin. Mech. Fluids, Heat*, vol. 6, no. 3, pp. 79–88, 2010.

[23] S. Abdullah, N. Ismail, M. Z. Nuawi, M. Z. Nopiah, and A. Ariffin, "Using the Hybrid Kurtosis-based Method to Correlate Strain and Vibration Signals," *WSEAS Trans. Signal Process.*, vol. 6, no. 3, pp. 79–90, 2010.

[24] R. B. Randall and J. Antoni, "Rolling element bearing diagnostics-A tutorial," *Mech. Syst. Signal Process.*, vol. 25, no. 2, pp. 485–520, 2011.